COMBINED RADIATION AND NATURAL CONVECTION IN PARTICIPATING LAMINAR FLOW OVER A VERTICAL CIRCULAR PIN

E. Khoshravan and G. Soleimani

Department of Mechanical Engineering
The University of Tabriz
Tabriz, Iran

Abstract The interaction of thermal radiation with conduction and laminar natural convection in a vertical circular pin, situated at participating gas, is numerically investigated. An absorbing and emitting gas is considered, and treated to be a gray participating media. Under the idealizing of gray gas, the *Rosseland* approximation is employed to describe the radiative heat flux in the energy equation. The modified box method with unequal grid spacing is used to perform the numerical computation of the coupled boundary layer conservation equations and pin conduction equation. The effects of buoyancy and radiation on the temperature, velocity, heat flux, and Nusselt number are examined in detail. The Nusselt number variation shows that heat transfer is enhanced by thermal radiation. Also, the local Nusselt number is found to be strongly dependent on the temperature ratio ψ_T, radiation-conduction parameter ψ_R, and conventional Gr and Pr numbers. Furthermore, the results are comparable with the available data in the literature for pure natural convection.

Key Words Natural convection, Conduction, Radiation, Participating Media, Heat Transfer, Finite Difference, Circular Pin

چکیده در این مقاله عکس العمل متقابل تابش حرارتی بارسانش و جابجائی آزاد آرام در جریان گاز سهیم از روی یک میله استوانه ای قائم بطور عددی بررسی شده است. گاز جذب کننده و گسیلنده در نظر گرفته شده و مثل یک محیط سهیم خاکستری عمل می کند. از تقریب روزلند برای بیان شار تابش حرارتی در معادله انرژی استفاده می شود. برای حل معادلات کوپله شده بقا در لایه مرزی و معادله رسانش حرارتی در میله روش اختلاف محدود باکس اصلاح شده با گره بندی نامساوی بکاربرده می شود. تاثیر شناوری و تابش بر روی توزیع دما، سرعت، شار گرما و عدد ناسلت بطور مفصل بررسی شده است. تغییرات عدد ناسلت کلی نشان می دهد که تابش حرارتی انتقال حرارت را بهبود می دهد. همچنین عدد ناسلت کلی بستگی شدیدی به نسبت دمای ψ_T ، پارامتر تابش-رسانش ψ_R ، عدد گراشف و عدد پرانتل دارد. نتایج بدست آمده در اینجا با نتایج موجود در ادبیات فن در مورد جابجائی تنها مقایسه شده و تطابق خوبی دیده می شود.

INTRODUCTION

Interaction of natural convection-radiation occurs in a variety of thermal engineering applications such as fins and cooling of electronic equipments. Research in conjugated convection-conduction heat transfer in fins has been reported in the literature. Sparrow and Acharya [1] and Sparrow and Chyu [2] analyzed conjugated convection-conduction problems for a vertical plate fin using finite difference method. In nonparticipating media, Sarma and Subrahmanyam [3] have studied the problem of combined convection radiation for a vertical plate by integral method. Hsu and Tsai [4] investigated the combined convection radiation interaction in a vertical plate fin situated in a participating gas. In the case of circular pin, Huang and Chen [5] and Huang et al. [6] have studied the conjugated forced convection-conduction and natural convection-conduction problems, respectively. They concluded that convective fin analysis based on a

uniform heat transfer coefficient value gave good prediction for overall heat transfer rate of the fin, yet could not accurately predict local heat flux. Lee et al. [7] considered natural convection along slender vertical cylinder with variable surface temperature. A number of studies have been reported on combined radiation convection in ducts and cavity, [8-14], but no work appears to be reported on the vertical circular pin in gray participating media. Therefore, the main objective of this article is to deal with heat transfer phenomena of a vertical circular pin subject to constant temperature at one end and heat loss from its side to participating ambient by radiation

ANALYSIS

Consider a homogeneous vertical circular pin (Figure 1) of radius r_o, which is extended from a wall at temperature T_o and situated in an otherwise quiescent participating media having temperature T_∞. Here if we assume $T_\infty < T_o$, the flow moves upward and the gravity **g** acts downard in the direction opposite to the flow. The circular pin loses heat from its side by natural convection and radiation. The properties of the fluid are assumed to be constant, except for the density variation that induces the buoyancy force, which is employed by the *Boussinesq* approximation

involves the divergence of the radiation flux $\nabla.q^r$, whereas the determination of the radiation flux q^r requires the medium temperature distribution. When energy transfer by radiation and convection is present, the law of conservation of energy becomes a complicated nonlinear integrodifferential equation. Since an exact analysis of the interaction of a radiation field with absorbing and emitting media in the laminar boundary layer is a very difficult problem, the *Rosseland* approximation, which is valid for intense absorption, is used to approximate the radiant energy flux. The *Rosseland* approximation for the radiative heat flux in an optically thick medium is given by [15]:

$$q^r = -\frac{4}{3\beta^*}\nabla e_b = -\frac{4\sigma}{3\beta^*}\nabla T^4 \qquad (4)$$

where β^* is the mean absorption coefficient, and σ is the Stefan-Boltzmann constant. Here we ignored the radiation in the axial direction in the energy equation. Hence the divergence of the radiation flux becomes:

$$\nabla.q^r = \frac{-4\sigma}{3\beta^*}\left[\frac{\partial^2 T^4}{\partial r^2} + \frac{1}{r}\frac{\partial T^4}{\partial r}\right] = \frac{-16\sigma}{3\beta^*}\frac{1}{r}\frac{\partial}{\partial r}\left(rT^3\frac{\partial T}{\partial r}\right) \qquad (5)$$

The corresponding boundary conditions of Equations 1-3 are:

$$r = r_0\ ,\ 0 < x < L\ ,\ u = v = 0\ ,\ T = T_w(x) \qquad (6\text{-a})$$

$$r \to \infty\ ,\ 0 < x < L\ ,\ u \to 0\ ,\ T \to T^\infty \qquad (6\text{-b})$$

$$x = 0\ ,\ r > r_0\ ,\ u = 0\ ,\ T = T_\infty \qquad (6\text{-c})$$

where $T_w(x)$ is the pin wall temperature. For a vertical circular pin with radius much smaller than its length, it can be assumed that heat transfer in the pin is mainly due to conduction in the longitudinal direction, so that a one-dimensional condition can be assumed for the pin energy equation. Thus, the energy equation for pin is given as:

$$\frac{d^2T_p(x)}{dx^2} - \frac{2h_t(x)}{k_p r_o}(T_p(x) - T_\infty) = 0 \qquad (7)$$

with

$$x = 0 \qquad T_p(x) = T_0 \qquad (8\text{-a})$$

$$x = L \qquad \frac{dT_p(x)}{dx} = 0 \qquad (8\text{-b})$$

where $T_p(x)$ is the pin temperature, k_p the pin thermal conductivity, L the length of the pin, and $h_t(x)$ the local combined radiation-convection heat transfer coefficient. The energy transport from the pin wall to the participating ambient in the presence of thermal radiation depends on two related factors: the fluid temperature gradient at the pin wall and the rate of radiative heat exchange. Hence, the wall heat flux, $q_w(x)$, at the pin surface can be expressed as:

$$q_w(x) = q_{conv}(x) + q_{rad}(x) \qquad (9\text{-a})$$

$$q_w(x) = h_t(x)\,(T_p(x) - T_\infty) \qquad (9\text{-b})$$

$$q_{conv}(x) = -k\left.\frac{\partial T(r,x)}{\partial r}\right|_{r = r_o} \qquad (9\text{-c})$$

$$q_{rad}(x) = -\frac{4\sigma}{3\beta^*}\left.\frac{\partial T^4(r,x)}{\partial r}\right|_{r = r_o} \qquad (9\text{-d})$$

where $q_{conv}(x)$ and $q_{rad}(x)$ represent the wall heat flux due to convection and radiation, respectively. The basic coupling for the thermal conjugate relationship between pin energy equation and boundary layer equations is expressed by the requirement that the fluid and the pin temperature and heat flux be continous along the pin-fluid interface, that is,

$$T_p(x) = T_w(x) \qquad (10)$$

$$h_t(x)\,(T_p(x) - T_\infty) = -k\frac{\partial T(r,x)}{\partial r}\bigg|_{r=r_o} - \frac{4\sigma}{3\beta^*}\frac{\partial T^4(r,x)}{\partial r}\bigg|_{r=r_o} \qquad (11)$$

Equations 1-3, 7, and 11 can be reduced to a system of dimensionless equations by introducing the following definitions:

$$X = \frac{x}{L}\ ,\ R = \frac{r}{L}Gr_L^{1/4}\ ,\ U = \frac{uL}{\nu}Gr_L^{-1/2}\ ,\ V = \frac{vL}{\nu}Gr_L^{-1/4}$$

$$\theta = \frac{T - T_\infty}{T_o - T_\infty}\ ,\ \theta_p = \frac{T_p - T_\infty}{T_o - T_\infty} \qquad (12)$$

where the Grashof number Gr_L is defined as:

$$Gr_L = \frac{g\beta\,(T_o - T_\infty)\,L^3}{\nu^2}$$

Introducing non-dimensional parameters (12) into Equations 1-3, 7, and 11 results in:

$$\frac{\partial(RU)}{\partial X} + \frac{\partial(RV)}{\partial R} = 0 \qquad (13)$$

$$U\frac{\partial U}{\partial X} + V\frac{\partial U}{\partial R} = \theta + \frac{1}{R}\frac{\partial}{\partial R}\left(R\frac{\partial U}{\partial R}\right) \qquad (14)$$

$$U\frac{\partial \theta}{\partial X} + V\frac{\partial \theta}{\partial R} = \frac{1}{Pr}\frac{1}{R}\frac{\partial}{\partial R}\left(R\frac{\partial \theta}{\partial R}\right) + \frac{\psi_R}{Pr}\frac{1}{R}\frac{\partial}{\partial R}\left[R(1 + \psi_T\,\theta)^3\frac{\partial \theta}{\partial R}\right] \qquad (15)$$

$$\frac{d^2\theta_p(X)}{\partial X^2} - 2h_t^+(X).\,\psi_C\,.\,\theta_p(X) = 0 \qquad (16)$$

where $Pr = \nu/\alpha$ is the Prandtl number, $\psi_R = 16\sigma T_\infty^3 / (3\beta^* k)$ the radiation-conduction parameter, $\psi_C = kLGr_L^{1/4} / (k_f r_o)$ the convection-conduction parameter, $\psi_T = (T_o - T_\infty)/T_\infty$ the temperature ratio, and $h_t^+(X) = h_t(x)\,L / (kGr_L^{1/4})$ the dimensionless local combined convection-radiation heat transfer coefficient. The transformed boundary conditions for fluid are:

$$R = R_o\ ,\ 0 < X < 1\ ,\ U = V = 0\ ,\ \theta = \theta_w(X)$$

$$R \to \infty\ ,\ 0 < X < 1\ ,\ U = 0\ ,\ \theta = 0$$

$$X = 0\ ,\ R > R_o\ ,\ U = 0\ ,\ \theta = 0 \qquad (17)$$

the corresponding conditions for the pin are:

$$X = 0 \qquad \theta_p(X) = 1 \qquad (18\text{-a})$$

$$X = L \qquad \frac{d\,\theta_p(X)}{d\,X} = 0 \qquad (18\text{-b})$$

The thermal coupling between the pin and the fluid can be transformed as follows:

$$\theta_p(X) = q_w(X) \qquad (19)$$

$$h_t^+(X) = \frac{1}{\theta_p(X)}\frac{\partial \theta(R,X)}{\partial R}\bigg|_{R=R_o} - \left[\frac{\psi_R}{\theta_p(X)}(1 + \psi_T\,\theta_p(X))^3\frac{\partial \theta(R,X)}{\partial R}\right]_{R=R_o} \qquad (20)$$

In the case of combined convection-radiation heat transfer, the local Nusselt number $Nu_t(x)$ is related to the total heat flux through the wall.

$$Nu_t(x) = Nu_{conv}(x) + Nu_{rad}(x) \qquad (21)$$

with

$$Nu_t(x) = \frac{h_t(x).L}{k}$$

$$Nu_{conv}(x) = -\frac{Gr_L^{1/4}}{\theta_p(X)}\frac{\partial \theta(R,X)}{\partial R}\bigg|_{R=R_o} \qquad (22)$$

$$Nu_{rad}(x) = -\frac{Gr_L^{1/4}\psi_R}{\theta_p(X)}(1 + \psi_T\theta_p(X))^3\frac{\partial \theta(R,X)}{\partial R}\bigg|_{R=R_o}$$

where $Nu_{conv}(x)$ and $Nu_{rad}(x)$ are convective and radiative Nusselt number respectively. Thus the formulation indicates that the local Nusselt number is governed by the following parameters:

$$Nu_t(x) = f(Gr, Pr, \psi_R, \psi_T, R_o)$$

where $R_o = r_o Gr_L^{1/4}/L$ is the pin parameter. The local combined convective-radiative heat flux can be taken as:

$$\frac{q_w(x).L}{k(T_o - T_\infty)\,Gr_L^{1/4}} = -\frac{\partial\theta(R,X)}{\partial R}\bigg|_{R=R_o} - \psi_R(1+\psi_T\theta)^3\frac{\partial\theta}{\partial R}\bigg|_{R=R_o} \qquad (23)$$

SOLUTION METHODOLOGY

In its overall pattern, the solution begins by solving the combined convection-radiation boundary layer problem for an isothermal circular pin with $T_p(x) = T_o$ (i.e., $\theta_p(X) = 1$) for all X. The dimensionless heat transfer coefficient $h_t^+(x)$ determined from this solution in accordance with Equation 20 are then used as input to the pin heat conduction Equation 16; but note that $\theta_p(X)$ which appears on the right-hand side of Equation 16 is treated as unknown (i.e., $\theta_p(X)$ from the boundary layer solution is not transferred to Equation 16). With prescribed values for ψ_C and ψ_R, the differential Equation 16 is then solved to yield $\theta_p(X)$. To begin the next cycle of the iterative procedure, the just-determined $\theta_p(X)$ is imposed as the thermal boundary condition for the combined convection-radiation boundary layer problem (Equations 13-15), the solution to which yields a new $h_t^+(x)$ distribution which is used as input to the pin heat conduction equation. This procedure of alternately solving the boundary layer problem and the pin conduction problem was continued until convergence was attained. To track the approach to convergence, the dimensionless total heat transfer coefficient $h_t^+(x)$ was monitored. When the cycle-to-cycle relative error was less than 10^{-4}, convergence was deemed to have been attained. The number of cycles needed for convergence ranged from four to ten, depending on the values of ψ_C and ψ_R. This rapid convergence validates the selection of the heat transfer coefficient ($h_t^+(x)$) as the transferred quantity from the boundary layer problem to the heat conduction problem. The boundary layer solutions were obtained by a marching procedure, starting at the leading edge where X=0 and proceeding downstream step-by-step until X=1 is reached. The boundary layer governing Equations 13-15 are discretized by fully implicit finite difference procedure based on modified box scheme. Together with boundary conditions (17) approximate solution in each marching step are obtained by Newton-Raphson iterative method. The grid pattern encompassed 60 grid points in the cross-stream (R) direction and 40 grid points in the streamwise (X) direction. There was a denser concentration of grid points near the leading edge (small X) to accommodate the initial rapid growth of the boundary layer. In addition, at all X, the grid points were more densely concentrated near the pin surface. For grid spacing, a constant ratio between two adjacent increments was used, that is:

$$\frac{\Delta R_{j+1}}{\Delta R_j} = k_1 \qquad \frac{\Delta X_{n+1}}{\Delta X_n} = k_2$$

where **j** and **n** are the grid location in **R** direction and marching step respectively. In this study, the suitable values for k_1 and k_2 are 1.0420 and 1.0422 respectively. At each marching step, convergence is assumed when the following convergence criterion is satisfied:

$$\frac{|\phi_z - \phi_{z-1}|}{|\phi_z|} \le 10^{-4} \qquad \text{for all } \phi$$

where ϕ refers to the any dependent variable (θ, U, V), z stands for the zth iteration. It is found in the separate computation that the difference in results obtained by using fully implicit finite difference scheme with 90×100 equally spaced grid points, and modified box method with 60×40 unequally spaced grid points are always less than 4 percent. Also the computation time for the modified box method is almost half of the computation time needed to perform the fully implicit scheme. When convergence temperature field is reached, the local Nusselt number and dimensionless heat flux can be calculated from Equations 21 and 23 respectively.

RESULTS AND DISCUSSION

In participating media, to demonstrate the behaviour of thermal characteristics of boundary layer using the *Rosseland* approximation for radiation model, the velocity, temperature, and local Nusselt number are found versus different radiation-conduction and convection-conduction parameters. Since the radiation and convection interaction is of primary concern here, all results are for fixed values of $\Delta X_1 = 0.01$, $\Delta R_1 = 0.09$, Pr = 0.76, $\psi_T = 0.5$, and $R_o = 2.8$. Figure 2 shows the effect of radiation-conduction parameter ψ_R on the dimensionless axial velocity at the boundary layer. The radiation-conduction parameter is defined as the ratio of radiation effect to conduction effect. The effect of radiation gets stronger as the ψ_R increases. With increased ψ_R, the distribution of axial velocity goes up. This implies that the presence of radiation effects tends to increase the effect of buoyancy. Also, the maximum value for velocity and momentum boundary layer thickness increases with radiation effect. Figure 3 represents the effects of convection-conduction parameter ψ_C on axial velocity distribution. The greater value of ψ_C indicates the smaller pin conductivity. Hence, at high value of ψ_c, temperature at any location along the pin reduces, and buoyancy effect decreases.

Figure 4 shows the temperature distribution in the boundary layer as a function of the dimensionless distance from the surface at X = 1 for different values of ψ_R. The temperature profile for $\psi_R = 0$ corresponds to nonradiating fluid. The maximum temperature in

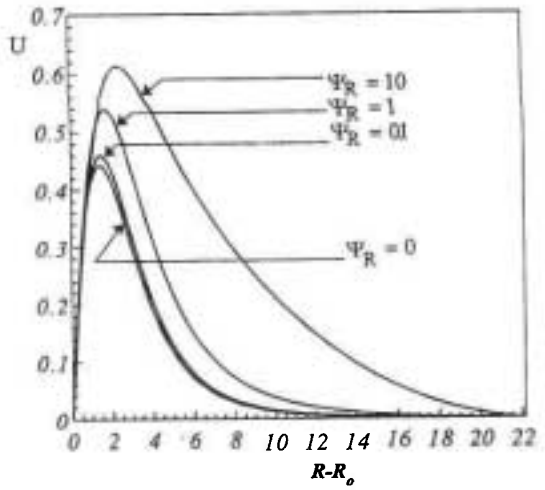

Figure 2. Effect of radiation-conduction parameter on dimensionless velocity profile in boundary layer, $\psi_C = 1.$, X = 1.

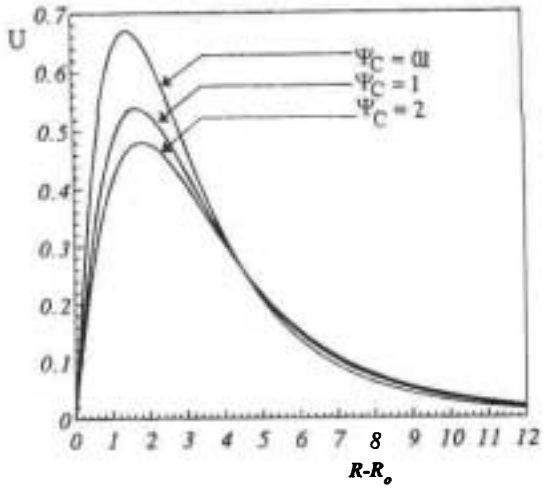

Figure 3. Effect of convection-conduction parameter on dimensionless velocity profile in boundary layer, $\psi_R = 1$, X = 1.

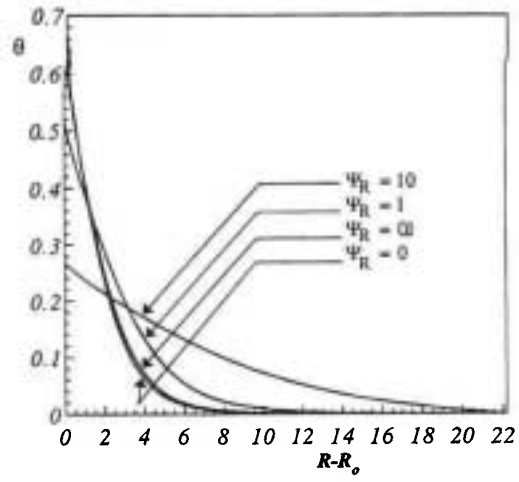

Figure 4. Effect of radiation-conduction parameter on dimensionless velocity profile in boundary layer, $\psi_C = 1$, X = 1.

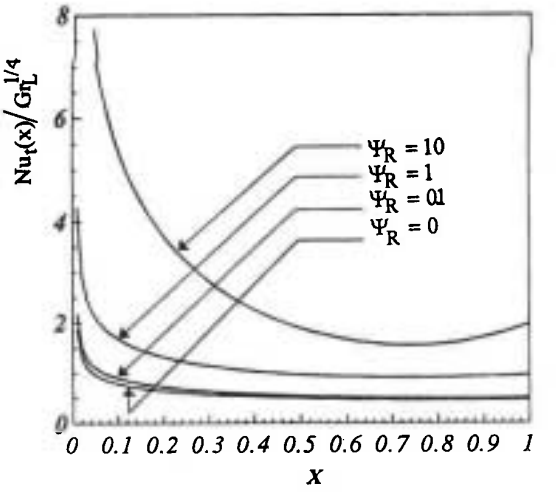

Figure 6. Effect of radiation-conduction parameter on Nusselt number for $\psi_C = 1$.

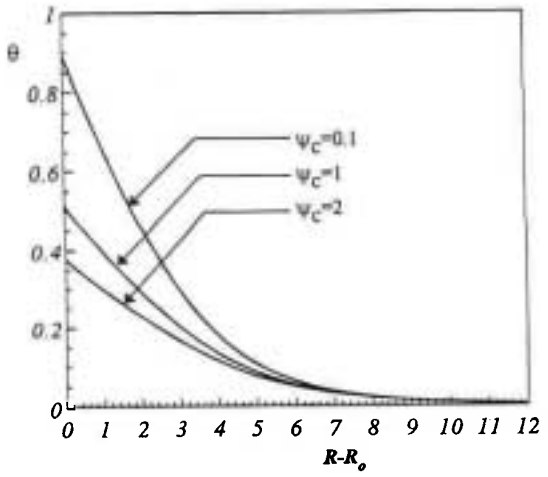

Figure 5. Effect of convection-conduction parameter on dimensionless velocity profile in boundary layer, $\psi_R = 1$, X = 1.

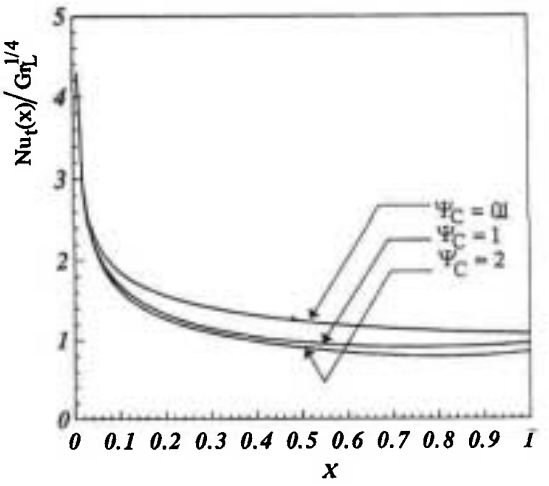

Figure 7. Effect of convection-conduction parameter on Nusselt number, $\psi_R = 1$.

the boundary layer is highest with the nonradiating fluid. The effect of radiation within the boundary layer is to flatten the temperature profile and hence to reduce the temperature. Figure 5 illustrates the distribution of temperature in boundary layer as a function of convection-conduction parameter ψ_C. The greater value of ψ_C (smaller pin conductance) gives the decreasing pin temperature and causes temperature gradient in fluid at boundary layer to decrease. Figure 6 shows the effect of ψ_R on the local Nusselt number. The solution without radiation ($\psi_R = 0$) is also shown for comparison. In all cases the $Nu_t(x)$ with radiation is larger than that without radiation. This is due to two effects. First, the radiation

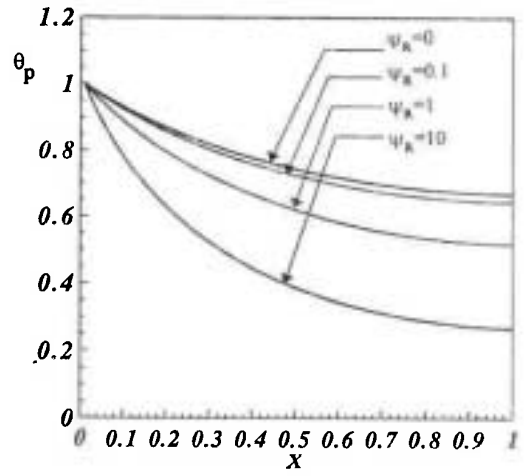

Figure 8. Effect of radiation-conduction parameter on dimensionless pin temperature distribution for $\psi_C = 1$.

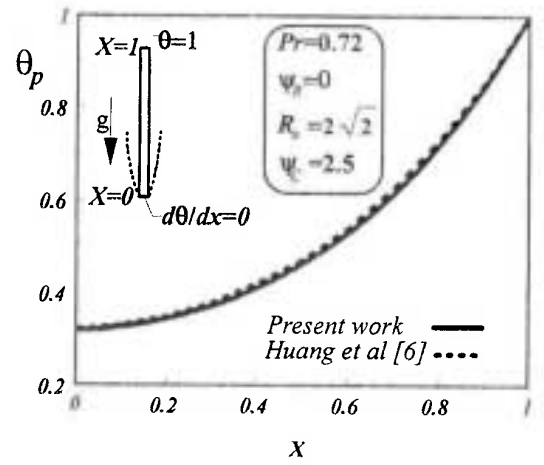

Figure 10. Dimensionless pin temperature distribution for pure convection.

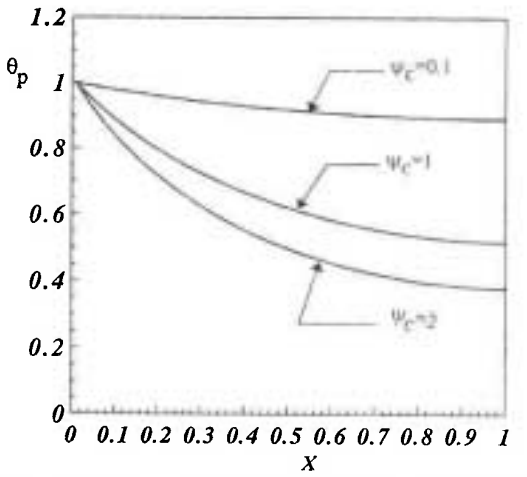

Figure 9. Effect of convection-conduction parameter on dimensionless pin temperature distribution for $\psi_R = 1$.

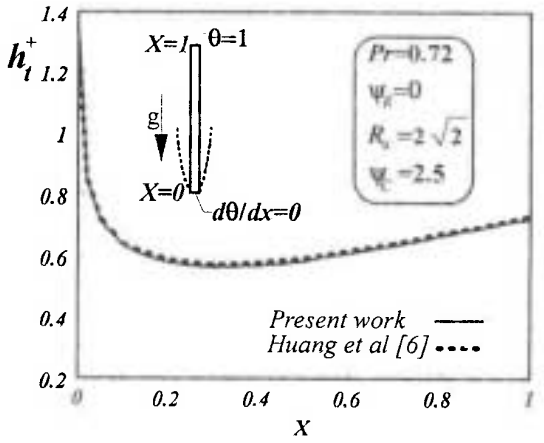

Figure 11. Dimensionless local heat transfer coefficient for pure convection.

is an additional mechanism for heat transfer through the gas resulting in an increased heat flux. Second, the radiation augments the velocity at boundary layer so that heat transfer increases with ψ_R. Both effects act to increase the local Nusselt number. Careful scrutiny on Figure 6 discloses that the curves with radiation tend to attain a minimum and then rise gradually. The location of these minima is shifted to small X as radiation increases. Additionally, it is found that the $Nu_t(x)$ increases with the increase in ψ_R. This is due to the stronger radiation interaction for the flow with large ψ_R. Figure 7 shows the dependence of the local Nusselt number on convection-conduction parameter ψ_C. The general trend of the curves shows that the local Nusselt number is characterised by an initial sharp drop, which becomes more gradual with increasing X. An increase in convection-conduction parameter, causes a drop in the local Nusselt number. This is due to the increasing temperature gradient in the pin. Since the temperature in the vicinity of the pin

root is higher than in other locations on the pin, it is seen that in the region near to the pin root, local Nusselt number increases.

To demonstrate the role played by the radiative loss mechanism, Figure 8 shows the effect of radiation interaction on the pin temperature profiles. It is clearly shown that as thermal radiation intensifies, heat flux from the pin surface increases, causing the pin temperature to decrease. Figure 9 shows the effect of convection-conduction parameter ψ_C on the pin temperature distribution. The Figure depicts the characteristic that larger values of ψ_C give rise to larger pin temperature variations, which shows the expected trend. To verify the accuracy of the present work, results of these calculations for pure convection are shown in Figures 10 and 11. Comparison of these curves shows reasonable agreement between the results of M. J. Huang et al. [6] and those of present work.

CONCLUSIONS

Combined laminar natural convection and radiation heat transfer of an absorbing-emitting gas over a vertical circular pin have been investigated in this research. Radiation by the participating gas has been modelled by *Rosseland* approximation. The local heat transfer coefficient along the pin is simultaneously solved for combined natural convection-radiation boundary layer equations of the fluid and the energy equation of the pin. A fully implicit box technique is employed. The effects of convective and radiative parameter on thermal behaviour of system are presented. To summarize, the following conclusions are drawn.

1. The thicknesses of the momentum and thermal boundary layer and the maximum velocity of the fluid increase as the radiation heat transfer becomes more dominant. This leads to the conclusion that as the radiation heat transfer becomes dominant, the heat flux distribution becomes more evenly spread out in the fluid boundary layer.

2. Temperature distribution in the gas flow is affected by the radiation effect. The effect is small when the radiation interaction is small.

3. With increases in radiation-conduction parameter, the $Nu_t(x)$ is enhanced as a result of greater radiation effect.

4. Results of these calculations for pure convection agree very well with those of previous investigations.

NOMENCLATURE

e_b	black body emissive power
g	acceleration of gravity
Gr	Grashof number
$h_t(x)$	combined radiation-convection heat transfer coefficient
$h_t^+(x)$	dimensionless combined radiation-convection heat transfer coefficient
k	fluid thermal conductivity
k_p	pin thermal conductivity
L	pin length
$Nu_{conv}(x)$	convective Nusselt number
$Nu_{rad}(x)$	radiative Nusselt number
$Nu_t(x)$	local Nusselt number
Pr	Prandtl number
q^r	radiation flux vector
$q_{conv}(x)$	convective heat flux from pin wall
$q_{rad}(x)$	radiative heat flux from pin wall
$q_w(x)$	total heat flux from pin wall
r	radial coordinate
r_o	radius of pin
R	dimensionless radial coordinate
R_o	pin parameter
T	fluid temperature
T_p	pin temperature
T_o	root temperature of pin
T_w	pin wall temperature
T_∞	ambient temperature

u	axial velocity
U	dimensionless axial velocity
v	radial velocity
V	dimensionless radial velocity
x	axial coordinate
X	dimensionless axial coordinate
α	fluid thermal diffusivity
β	thermal expansion coefficient
β^*	mean absorption coefficient
θ	dimensionless temperature of fluid
θ_p	dimensionless temperature of pin
ν	kinematic viscosity
σ	Stefan-Boltzmann constant
ψ_C	convection-conduction parameter
ψ_R	radiation-conduction parameter
ψ_T	temperature ratio

REFERENCES

1. E. M. Sparrow and S. Acharya, "A Natural Convection Fin with a Solution-Determined Nonmonotonically Varying Heat Transfer Coefficient," *ASME Journal of Heat Transfer*, Vol. 103, (1981), 218-225.
2. E. M. Sparrow and M. K. Chyu, "Conjugate Forced Convection-conduction Analysis of Heat Transfer in a Plate Fin," *ASME Journal of Heat Transfer*, Vol. 104, (1982), 204-206.
3. P. K. Samara and T. Subrahmanyam, "Turbulent Free Convection from a Radiating Vertical Surface Situated in Air-A Conjugate Problem," *Int. Comm. Heat Mass Transfer*, Vol. 16, (1989), 883-894.
4. T. H. Hsu and S. Y. Tsai, "Thermal Response of a Heated Vertical Plate Fin with Natural Convection-Radiation Interaction," Numerical Heat Transfer, Part A, Vol. 22, (1992), 307-322.
5. M. J. Huang and C. K. Chen, "Vertical Circular Pin with Conjugate Forced Convection-Conduction Flow," *ASME Journal of Heat Transfer*, Vol. 106, (1984), 658-661.
6. M. J. Huang, C. K. Chen and J. W. Cleaver, "Vertical Circular Pin with Conjugated Natural Convection-Conduction Flow," *ASME Journal of Heat Transfer*, Vol. 107, (1985), 242-245.
7. H. R. Lee, T. S. Chen and B. F. Armaly, "Natural Convection Along Slender Vertical Cylinders with Variable Surface Temperature," *ASME Journal of Heat Transfer*, Vol. 110, (1988), 103-108.
8. J. R. Tsai, M. N. Ozisik, "Combined Convection and Radiation in Participating Laminar Flow inside a Parallel-Plate Duct with Flux Boundary Condition," *Int. Comm. Heat Mass Transfer*, Vol. 16, (1989), 861-874.
9. L. K. Yang, "Combined Mixed Convection and Radiation in a Vertical Pipe," *Int. Comm. Heat Mass Transfer*, Vol. 18, (1991), 419-430.
10. L. K. Yang, "Forced Convection in a Vertical Pipe with Combined Buoyancy and Radiation Effects," *Int. Comm. Heat Mass Transfer*, Vol. 19, (1992), 249-262.
11. G. Yang, M. A. Ebadian and A. Campo, "A Numerical Study of Convective and Radiative Transfer in Ducts of Rectangular and Equilateral Cross Sections," *Int. J. Heat Mass Transfer*, Vol. 34, No. 4/5, (1991), 1319-1322.
12. Z. F. Dong and M. A. Ebadian, "Convective and Radiative Heat Transfer in the Entrance Region of an Elliptic Duct with Fins," *Numerical Heat Transfer*, Part A, Vol. 21, 1992, 91-107.
13. C. Balaji and S. P. Venkanteshan, "Natural Convection in L Corners with Surface Radiation and Conduction," *ASME Journal of Heat Transfer*, Vol. 118, (1996), 222-225.
14. A. A. Dehghan and M. Behnia, " Combined Natural Convection-Conduction and Radiation Heat Transfer in a Discretely Heated Open Cavity," *ASME Journal of Heat Transfer*, Vol. 118, (1996), 56-64.
15. R. Viskanta, "Radiation Heat Transfer: Interaction with Conduction and Convection and Approximate Methods in Radiation," Proc. 7th Int. Heat Transfer Conf., U. Grigull, E. Hahne, K. Stephan and J. Straub, eds., Vol. 1, (1982), 103-122.